Article

Investigation of Microscale Periodic Ni-Mg-Ni-Mg Film Structures as Metal-Hydride Hydrogen Accumulators

Alexander G. Ivanov, Dmitri A. Karpov *, Evgeniy S. Chebukov and Michael I. Yurchenkov

JSC "NIIEFA", Doroga na Metallostroy, 3, Metallostroy, 196641 Saint Petersburg, Russia
* Correspondence: karpov@niiefa.spb.su

Abstract: Here, the authors report the results of their study on the key characteristics of microscale periodic Ni-Mg-Ni-Mg film structures as metal-hydride hydrogen accumulators, namely, the microstructure, phase state, operation temperatures and rate of the sorption/desorption processes, complete and reversible mass content of hydrogen, and enthalpy of metal hydrides' phase-formation. The study has shown that hydride-formation films can be saturated with up to 7.0–7.5 wt.% of hydrogen at pressures up to 30 atm and temperatures of 200–250 °C, with a reversible amount of stored hydrogen up to 3.4 wt.% during its desorption at a pressure of 1 atm and temperatures of 250–300 °C with the phase-formation enthalpy in the range of 19.8–46.7 kJ/mol H_2 depending on the nickel content (the thickness of the nickel layer). Structural and constructive schemes are proposed for film metal-hydride hydrogen accumulators for various applications of the hydrogen power industry.

Keywords: metal hydride; hydrogen accumulator; Ni-Mg-Ni-Mg film structure; X-ray diffraction analysis; sorption/desorption process; mass content of hydrogen; phase-formation enthalpy

1. Introduction

Nowadays, metal-hydride hydrogen storage systems are considered as promising ones for hydrogen transport, lifting and handling equipment, autonomous devices, backup and emergency power supply, etc. [1–4]. They favorably differ from alternative storage systems (liquid-state or high-pressure cylinders) by the higher packing density of hydrogen atoms, safety, the absence of leaks, and the low energy costs of hydride synthesis. The main disadvantage of metal-hydride systems is the presence of a metal matrix, which significantly increases the gravimetric density of these hydrogen storage systems. At present, LaNi$_5$ powders are mainly used in commercially available metal-hydride hydrogen accumulators [5–7]. Their advantages are the low temperature of the sorption/desorption processes (from room temperature to ~100 °C) and the low value of phase-formation enthalpy (31 kJ/mol H_2); their disadvantage is the low mass content of hydrogen (no more than 1.8%). Metal hydrides based on Mg alloys, wherein the mass content of hydrogen may be as high as 7.6% [8,9], would be more effective for practical application. However, there are serious barriers to the realization of this: the high temperature (300–350 °C) and low kinetics of sorption/desorption processes and high values of the phase-formation enthalpy (76 kJ/mol H_2) and energy consumption for activation. These barriers can essentially be mitigated by reducing the dispersion of powder (to the nanoscale) and using special technologies to grind them [10–13]. Another approach consists of the use of amorphous (nanoscale) films deposited in one way or another instead of bulk powder material [14,15]. As shown theoretically [16] and verified experimentally [17], the thinner a film, the better its thermodynamics and the lower the temperature of the sorption/desorption processes. As reported in [18], a hydrogen mass content of 5.58 wt.% was attained at a desorption temperature of 230 °C on multilayer nano-size (from 300 nm to 800 nm) Mg/Fe films with a protective Pd coating deposited via the method of resistive heating on polyimide

substrates. Fe films alternating with Mg films served as mechanically stable interlayers with a high value of hydrogen diffusion therein without producing hydrides at moderate temperatures and pressure. In addition, as is known, minor additives of Fe for powder materials improve the desorption characteristics of MgH_2 [19,20]. However, from the PCT diagrams presented in this work at a temperature of 200 °C, it follows that the mass content of hydrogen (5.56 wt.%) obtained at a pressure of ~9 atm is not reversible: when the pressure drops to ~2 atm (no measurements were carried out at lower pressures), the yield of hydrogen was only ~2 wt.%. Multilayer nano-size (from 50 nm to 500 nm) amorphous films obtained via the method of magnetron sputtering with alternating Mg85Ni14Ce1 and Pd layers were studied in [14]. It was shown that such sandwich-like structures can reversely absorb and desorb hydrogen at a temperature of 120 °C with an excellent capacity for cycling (however, with a reverse mass content of hydrogen only to 1.4 wt.% and desorption at a pressure of 10 Pa). In [21], a nanoscale Mg/Ni sandwich-like film structure was experimentally investigated for the first time, in which the Ni film (4 nm thick) served to protect against oxidation for the dissociation of H_2 molecules and as a catalyst for the hydrogenation of the Mg film (340 nm thick). As these experiments have shown, when hydrogenated for 1 h at room temperature and a hydrogen pressure of ~1 atm, the hydride fraction (the ratio of hydrogen atoms absorbed by magnesium to the total number of magnesium atoms) reached 0.35, and its maximum value (close to 1.0) was recorded at a magnesium film thickness of ~100 nm, falling sharply in the direction of tungsten substrate. With an increase in the hydrogenation time under the same conditions to 42 h, the peak value of the hydride fraction at a magnesium film thickness of ~100 nm increased to a value close to full hydrogenation with the same sharp decline to the substrate. Ni has worse solubility of hydrogen compared to Pd and is a less effective means of delivering it to the interface with Mg; however, this can be compensated for by an increase in hydrogenation pressure. In addition, a theoretical study of the absorption characteristics of hydrogen by the Mg/Ni interface through the analysis of electronic structures showed that the presence of the Mg/Ni interface improves the hydrogenation properties of Mg/Ni film systems, with a significant role of Ni in the adsorption of H atoms due to its stronger binding interaction with hydrogen [22]. Additionally, taking into account its high catalytic activity, the availability and cheapness of Ni leave no other alternative for practical applications of hydrogen energy. Our previous studies of thicker (microscale) Mg/Ni film structures (Mg ~5 microns with 200–400 nm Ni coating) [23] have shown the possibility of achieving sufficiently high sorption/desorption characteristics of hydrogen on them: the mass content of hydrogen was up to 5.4 wt.% (at sorption pressure of ~5 atm and desorption in vacuum conditions) without significant changes with subsequent oversaturation, the temperature peaks of desorption were reduced to 150–200 °C, and the hydrogen release time was reduced to ~20 min. The presence of a Ni coating demonstrated considerable improvements in hydrogen saturation and the kinetics of sorption/desorption processes in these micro-sized Mg/Ni films compared to the same films without a Ni coating. The results obtained have encouraged the current more detailed investigations of microscaled periodic Ni-Mg-Ni-Mg film structures as film metal-hydride hydrogen accumulators, the competitiveness of which is determined by the following main characteristics: reversible mass content of hydrogen at a desorption pressure of ~1 atm; the temperature and kinetics of sorption/desorption processes; the value of phase formation enthalpy, which determines the energy costs for decomposition of hydrides, as well as the cost and availability of the materials used. The paper investigates the key characteristics of microscaled periodic Ni-Mg-Ni-Mg film structures: microstructure, phase state, operating temperatures and rates of sorption/desorption processes; complete and reversible mass content of hydrogen (at a desorption pressure of ~1 atm); and enthalpy of the phase formation of metal hydrides. Based on the results attained, a possible constructive scheme of a film metal-hydride hydrogen accumulator based on periodic Ni-Mg-Ni-Mg film structures deposited on a polymer carrier with a resistive layer is proposed for practical applications.

2. Materials and Methods

Ni-Mg-Ni-Mg film structures were deposited in vacuum chamber 1 of the PLASMATECH-M facility of JSC NIIEFA (Figure 1) under vacuum conditions in Ar medium (at pressure of 0.5 Pa) using two magnetrons 2,3 with the sequential sputtering of targets of Mg (99.95%) and Ni (99.95%) with the final layer of Ni. The diameter of the targets was 100 mm, the thickness of the Mg target was 8 mm, and the thickness of the Ni target was 4 mm. The smaller thickness of the Ni target was associated with providing the necessary magnitude of the magnetic field on the surface of the ferromagnetic material. The sputtering of targets was carried out via the HIPIMS method (by means of high-power pulses). The sputtering time of the magnetron with a magnesium target was 30–35 min per layer at its power of 300 W. The sputtering time of a magnetron with a nickel target was 4–5 min per layer at the same power of 300 W.
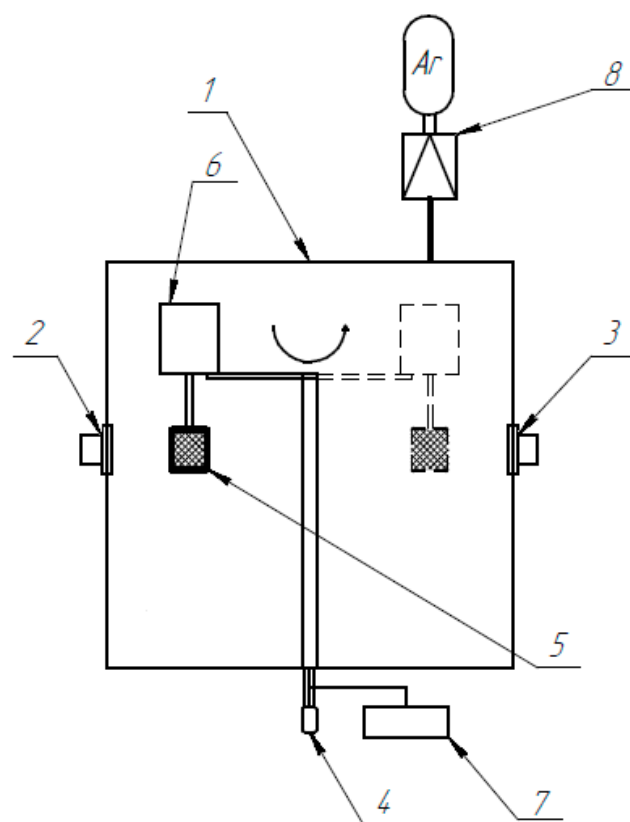
Figure 1. Diagram of the PLASMATECH-M facility: 1—vacuum chamber; 2—magnetron with magnesium target; 3—magnetron with nickel target; 4—rotation drive; 5—cylindrical shell; 6—stepper motor; 7—bipolar bias voltage power supply; 8—gas flow regulator (argon).

ПМ-1ЭУ polyimide film, which was 12.5 μm in thickness, was used as a substrate. The following stages of the preliminary preparation of the substrates were carried out: washing in an ultrasonic bath in purified gasoline for 20 min, washing in distilled water, and drying in a drying cabinet at a temperature of 80 °C. After preliminary preparation, the substrates were installed in the vacuum chamber of the facility and degassed in vacuum conditions at a temperature of 200 °C for 8 h. After degassing, the substrates were cleaned and activated in a glow discharge in an argon medium for 30 min while a bipolar bias voltage was applied to them.

A sufficiently large number of samples was required to provide a full cycle of experiments. For their production, polyimide tape was used, which was wound on cylindrical shell 5, which was made of stainless steel with a diameter of 75 mm and a height of 90 mm (placed on the shaft of stepper motor 6). Herewith, the stepper

motor was fixed on the bracket of rotation drive 4 with a shaft located along the axis of the vacuum chamber. To apply layer-by-layer films, a cylindrical shell was placed opposite one of the magnetrons and rotated around its axis using a stepper motor. After applying the appropriate layer, the cylindrical shell was exposed opposite another magnetron, and the next layer of the film structure was applied, and so on, until a predetermined number of layers was applied. For subsequent studies of the Ni-Mg-Ni-Mg film structures deposited in this way, the resulting tape was cut into samples of the required size. The mass of hydride-forming films in samples obtained in this way was in the range of 2–5 mg.

The saturation of the samples with hydrogen (purity > 99.999%) was carried out via the Sieverts method on the AKNDM automated complex of JSC NIIEFA (with pressure up to 50 atm and temperature up to 950 °C). The thermal desorption analysis of saturated samples was also carried out here. The internal dimensions of the measuring chamber of the complex were a diameter of 20 mm and a length of 20 mm. For the analysis, the sample was placed in the chamber located in the controlled heating furnace. The complex made it possible to determine the amount of desorbed hydrogen by the equation of state of the gas, taking into account the compressibility factor. The error in determining the pressure was ±2%, and the temperature was ±20 °C. The complex was calibrated according to the standard $LaNi_5$ powder sample and allowed the mass content of hydrogen in the sample to be determined with a relative accuracy of at least ±10%.

The microstructure of the films was studied using a Phenom 3G ProX scanning electron microscope (Phenom-World B.V., Eindhoven, The Netherlands) with an attachment for the analysis of the energy dispersion spectrum. The samples were poured into resin and then polished according to their cross-section. A holder for non-conducting samples was used for microstructural studies.

X-ray diffraction analysis (XRD) before and after hydrogen saturation was carried out using a DRON-8 diffractometer equipped with a Mythen 2R linear position-sensitive detector (Dectris Ltd., Baden-Dättwil, Switzerland). Diffraction patterns were recorded at the following parameters: angle range of 2θ–20—100°; scanning speed—1°/min; scanning step—0.1°; exposure time at the point—3 s; voltage—40 kV; current—20 mA. The analysis of diffractograms and phase identification was carried out using the COD database and the DrWin program (LECO Corporation, St. Joseph, MI, USA, software version: 6.00.95, 09.2009).

To determine the absolute hydrogen content in the films, a LECO RHEN602 analyzer was used. This device allows the user to determine the presence of hydrogen in samples when they are burned in a carbon crucible in an inert gas stream (argon). The released hydrogen passes through the filter system (chromatographic column) and enters the thermal conductivity cell. By changing the thermal conductivity of the gas flow, the hydrogen content in a sample is determined with an accuracy of 2% of the measured value. The 502-706-HAZ standard (titanium hydride powder) is used for calibration. To determine the mass content of hydrogen saturated, desorbed, or passed through colorimetric analysis, Ni-Mg-Ni-Mg film structures were separated from the substrate and placed in the crucible of the device. The mass of the analyzed samples of film structures was in the range of 2–5 mg.

Calorimetric analysis (determination of the enthalpy of hydride phase formation) was carried out using a DSC 3 Mettler-Toledo (Mettler-Toledo, Columbus, OH, USA) differential scanning calorimeter. The essence of the method is to compare the temperature of the analyzed crucible (with the sample) with the temperature of the comparison crucible when they are heated at a constant rate.

The device allows the temperature peaks of phase formation reactions to be determined with an absolute error of ±0.5 °C, as well as the specific heat of phase formation with a relative error of ±2.5%. During the analysis, a constant heating rate of 5 °C/min was maintained at an initial temperature of 150 °C and a final temperature of 350 °C. Standard aluminum crucibles with a lid with a volume of 100 μL were used. Argon with a flow

of 30–50 slm was used as a purge gas. To determine the enthalpy of the formation of the hydride phase, Ni-Mg-Ni-Mg film structures were separated from the substrate and placed in the crucible of the device. The mass of the analyzed samples of film structures was in the range of 1.5–4 mg.

3. Results

Table 1 presents the list of samples showing the compositions and parameters of the films deposited by the magnetron sputtering.

Table 1. List of samples.

| Sample	Sputtering Method	Layer Thickness, μm		Q-ty of Layers		Ni Protection Layer	Mg/Ni ratio, at.%
		Mg	Ni	Mg	Ni		
Mg/Ni1	Layer-by-layer	1.4	0.25	5	6	+	96/4
Mg/Ni2	Layer-by-layer	1.8	0.34	5	6	+	92/8
Mg/Ni3	Layer-by-layer	1.3	0.35	5	6	+	88/12

Figure 2 shows the sample of the microstructure of the deposited films (Mg/Ni2 sample).
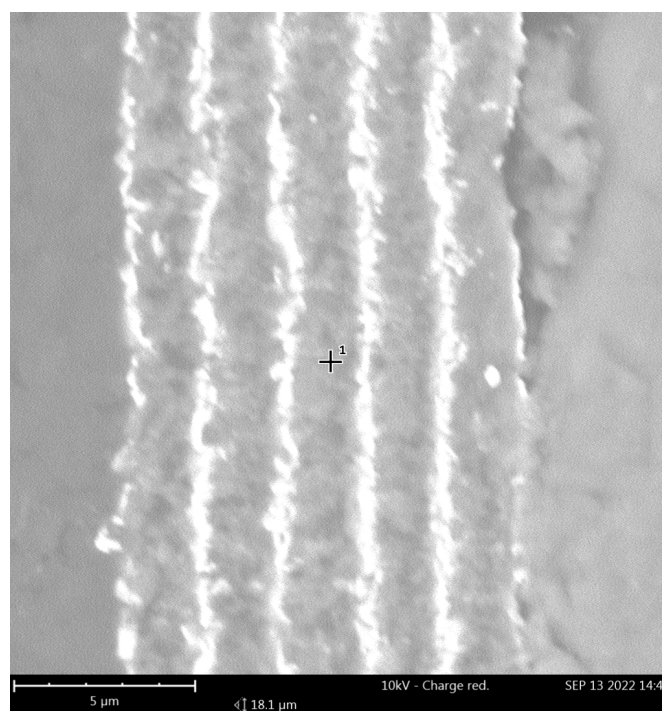
Figure 2. Sample of the microstructure of deposited films (Mg/Ni2 sample).

The image analysis shows that the films had an amorphous structure and good adhesion to the polyimide substrate, since the interface did not have any defects or delaminations.

The samples were saturated with hydrogen in the pressure range of 10–30 atm and temperature range of 200–300 °C for 4 h. Figure 3 shows the dependence of the hydrogen mass content on the saturation pressure at a temperature of 300 °C.
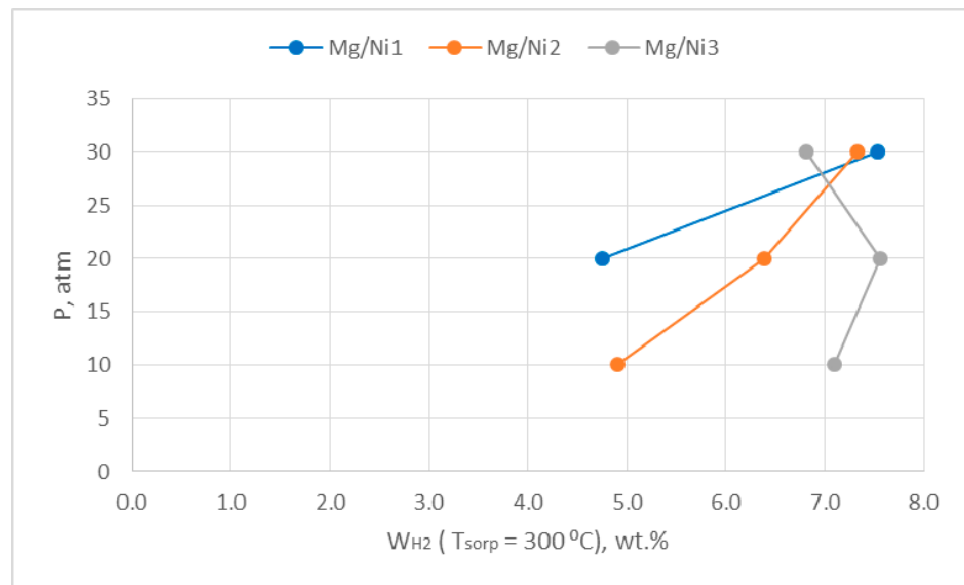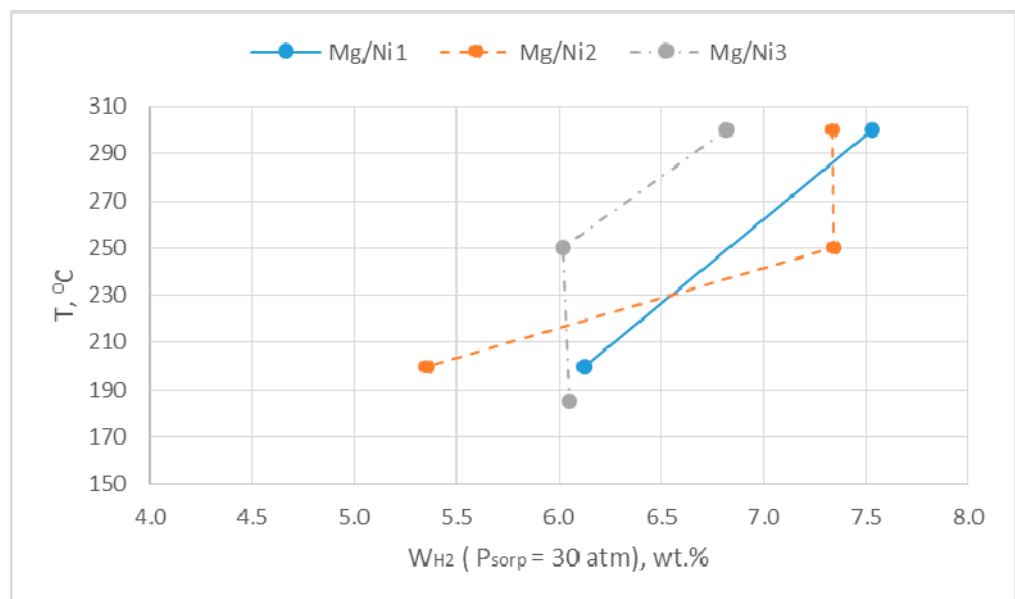
Figure 3. Dependences of the hydrogen mass content (W_{H2}) on the saturation pressure (P) at a saturation temperature (T_{sorp}) of 300 °C.

The mass content of hydrogen in the samples was determined on the LECO RHEN602 analyzer after their corresponding saturation on the AKNDM complex.

As can be seen from Figure 3, a sufficiently high value of the mass content of hydrogen was already achieved on the samples at a saturation pressure of 10 atm (Mg/Ni2: 4.9 wt.%; Mg/Ni3: 7.1 wt.%). It is interesting to note that an increase in saturation pressure was not always accompanied by an increase in the mass content of hydrogen: on Mg/Ni3 samples at a saturation pressure of 20 atm, the mass content of hydrogen was 7.6 wt.%, and at a saturation pressure of 30 atm—6.8 wt.%.

Figure 4 shows the dependences of the hydrogen mass content on the saturation temperature at a saturation pressure of 30 atm.


Figure 4. Dependences of the hydrogen mass content (W_{H2}) on the saturation temperature (T) at a saturation pressure (P_{sorp}) of 30 atm.

As can be seen from Figure 4, a sufficiently high value of the mass content of hydrogen was already achieved on samples at a temperature of ~200 °C (Mg/Ni1: 6.1 wt.%, Mg/Ni2: 5.3 wt.%, Mg/Ni3: 6.0 wt.%) with its growth when the temperature rose to 300 °C.

Figure 5 shows the results of the X-ray diffraction analysis of the samples before and after saturation. The most intensive was the magnesium peak. The relative intensity of the nickel peak increased from Mg/Ni1 to Mg/Ni3. Peaks of magnesium hydride and Mg_2NiH_4 intermetallide hydride were observed in the saturated samples. The signal of the Mg_2NiH_4 intermetallide hydride also increased from Mg/Ni1 to Mg/Ni3. The intensive signal corresponding to $\Theta = 29.4°$ was not found in the available database. The signals $\Theta = 47.5°$ and $48.4°$ were related to the composition fixing the samples on the object table of the diffractometer.
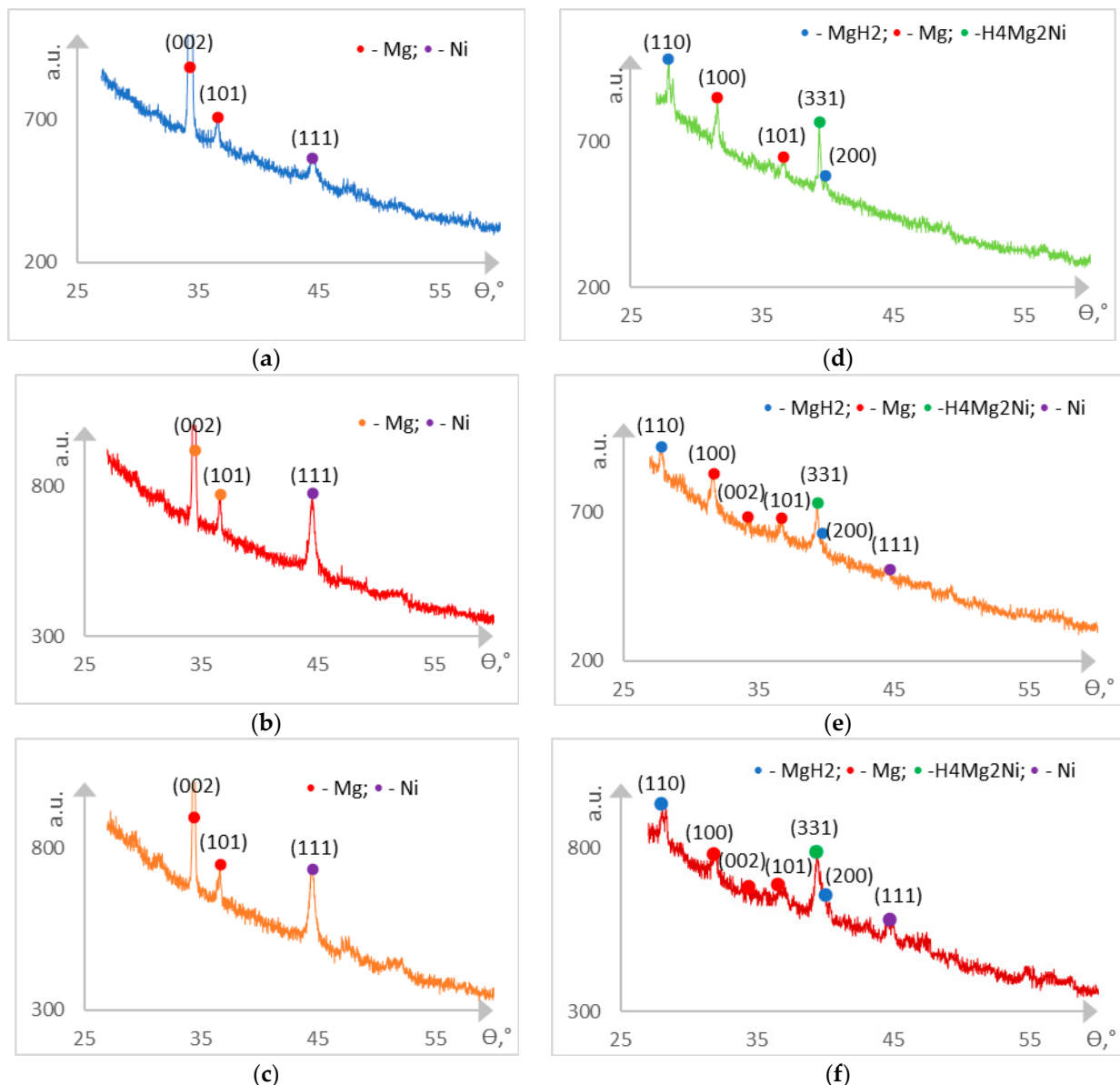
Figure 5. X-ray diffraction analysis of samples: before saturation: (**a**) Mg/Ni1; (**b**) Mg/Ni2; (**c**) Mg/Ni3; after saturation: (**d**) Mg/Ni1; (**e**) Mg/Ni2; (**f**) Mg/Ni3.

Table 2 presents the mass fractions of hydrides in the saturated samples at a temperature of 300 °C and a hydrogen pressure of 30 atm.

Table 2. Mass fractions of hydrides.

wt.%	Mg/Ni1	Mg/Ni2	Mg/Ni3
MgH_2	80.3	76.3	61.7
Mg_2NiH_4	13.5	15.1	36.3

A distinctly higher proportion of Mg_2NiH_4 phase in the Mg/Ni3 series sample was noteworthy.

The calorimetric analysis of the samples was performed at a heating rate of 5 °C/min from 150 °C to 350 °C in the argon atmosphere. Figure 6 presents the calorimetry results. Two thermal peaks were seen on all curves at a temperature of 240 °C and 270–300 °C. For the Mg/Ni3 sample, two peaks of 265 °C and 300 °C were seen instead of one high-temperature peak. The area of the 240 °C peak grew with an increase in the nickel dose, but the area of the high-temperature peak(-s) continued to prevailing.
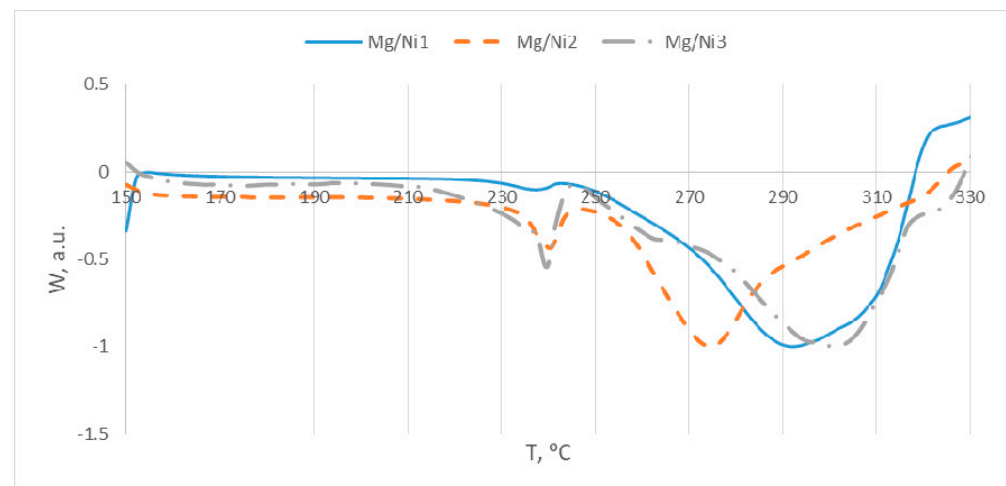
Figure 6. Calorimetric curves of the samples.

In practical applications (for example, in hydrogen fuel cells), the supply of hydrogen should occur, as a rule, at a pressure of ~1 atm and more. Therefore, in addition to the complete stored mass content of hydrogen in Ni-Mg-Ni-Mg film structures, its reversible-stored amount was studied; that is, the mass amount of hydrogen desorbed from hydrogen-saturated Ni-Mg-Ni-Mg film structures at a pressure of 1 atm. To achieve this, saturated samples were placed in the chamber of the AKNDM complex, a hydrogen pressure equal to one atmosphere was set in the chamber, and the samples were heated to a predetermined temperature (within 300 °C). When the pressure increased during desorption, part of the gas was discharged into the calibrated volume of the complex to maintain the pressure in the chamber equal to one atmosphere in this way. The desorption procedure continued until the equilibrium state of the hydrogen concentration in the sample was reached, as evidenced by the constancy of the pressure in the chamber. The duration of the process was about 1 h.

Table 3 shows the results of measurements of the mass content of hydrogen and the calorimetric analysis of the samples. The mass content of hydrogen was measured in the samples both after their saturation at a temperature of 300 °C and pressure of 30 atm, and after desorption of hydrogen from them (at a hydrogen pressure of 1 atm and temperature of 300 °C). Thus, the mass content of reversibly stored hydrogen in the samples was determined. The values of the enthalpy of phase formation (the amount of heat spent on hydrogen output) were determined by the sum of the areas of all endothermic temperature peaks of desorption (Figure 6) and the difference in the mass content of hydrogen in the samples before and after the calorimetric analysis.

Table 3. Results of measurements of the mass hydrogen content and calorimetric analysis of the samples.

| Sample	W_{H2} after Saturation, wt.%	W_{H2} after Desorption, wt.%	DW_{H2} of Reversibly Stored, wt.%	E(dH), kJ/mol	Temperature of Desorption Peaks, °C	
Mg/Ni1	7.5	4.9	2.6	46.7	236.7	292.9
Mg/Ni2	7.2	4.3	2.9	31.9	240	275
Mg/Ni3	7.0	3.6	3.4	19.8	240.2	260/290–300

4. Discussion

The maximum hydrogen content achieved was 7.5% wt.% in the Mg/Ni1 sample with magnesium content of 96 at.% and nickel of 4 at.%. At the same time, the maximum amount of reversibly stored hydrogen amounted to 3.4 wt.% for the Mg/Ni3 sample with a magnesium content of 88 at.% and nickel content of 12 at.% (during hydrogen desorption at a pressure of 1 atm and a temperature of 300 °C), with a hydrogen content of 7.0 wt.% in the sample in the saturated state. Thus, despite the decreased content of hydrogen in the saturated state, its reversibly desorbed amount was not decreased with an increase in the amount of nickel in the sample (as the ratio of thicknesses of the nickel and magnesium layers increased). On the contrary, it increased, testifying that the nickel content has an essential impact on the kinetics of the desorption processes. The optimal ratio of the thicknesses of the nickel and magnesium layers ensuring the maximum reversible amount of desorbed hydrogen has not been found in these experiments. This should be studied in future work. The enthalpy of the phase formation of bulk magnesium hydride MgH_2 was 76 kJ/mol H_2; the enthalpy of the phase formation of Mg_2NiH_4 intermetallic hydride is estimated differently in different sources and is in the range of 30–60 kJ/mol H_2 [24]. The enthalpy of the phase formation for the Mg/Ni1, Mg/Ni2, and Mg/Ni3 samples measured in the experiments was 46.7, 31.9, and 19.8 kJ/mol H_2, respectively, and corresponded to the increase in the nickel content of 4, 8, and 12 at.%, respectively, in these samples. The high-temperature peaks of Mg/Ni1 (290 °C), Mg/Ni2 (275 °C), and Mg/Ni3 (300 °C) corresponded to the decomposition of magnesium hydride. The low-temperature peaks of Mg/Ni1 (235 °C), Mg/Ni2 (237 °C), and Mg/Ni3 (237 °C), as well as the additional low-temperature peak of Mg/Ni3 (262 °C), were presumably associated with the decomposition of Mg_2NiH_4.

As is known from the literature, Mg_2NiH_4 intermetallide hydride undergoes a transition from the cubic to monoclinic phase at temperatures of 210–260 °C [25], and equilibrium pressure of hydrogen during its desorption from Mg_2NiH_4 in the temperature range of 300–350 °C amounts to 3.3–10.0 atm [26]. The presence of three peaks in the obtained calorimetric graphs of Mg/Ni3 can be interpreted using the three states of phase transformations with a rising temperature: the transition of Mg_2NiH_4 intermetallide from the cubic to monoclinic phase (240 °C), the decomposition of intermetallide hydride (265 °C), and the decomposition of magnesium hydride (300 °C). However, it should be noted that the unambiguous identification of low-temperature peaks of Mg_2NiH_4 decomposition requires additional X-ray studies. In all cases, the temperature of hydrogen desorption from the film metal-hydride samples was no more than 300 °C, which was considerably lower than the values for powder magnesium hydride (~350 °C).

The results of the presented experiments show that the use of microscale periodic Ni-Mg-Ni-Mg film structures causes higher sorption–desorption characteristics for the accumulation and yield of hydrogen and a lower enthalpy of phase formation compared with bulk powder materials. As well as recently studied Mg-Fe-Mg-Fe nanoscale film structures with a protective Pd coating and nanoscale film structures with alternating $Mg85Ni14Ce1$ and Pd layers [14,18], they are able to work effectively as a hydrogen accumulator, but without using expensive materials in their composition. Their use as metal-hydride hydrogen accumulators can be energetically more efficient than the use of powders based on both Mg and $LaNi_5$ intermetallic compounds. Figure 7 shows the

structural and constructive schemes of such a film metal-hydride accumulator, which is a development of its previously proposed versions [27,28]. It is made as a periodic Ni/Mg/Ni/Mg film structure consisting of alternating layers of Ni and Mg deposited on a polymer substrate with a resistive layer. The accumulator is charged (hydrogen sorption) and discharged (hydrogen desorption) during the heating of the film structure by current passing through the resistive layer. This practically inertialess and uniform heating of the film structure compares favorably with the rather inertial and nonuniform heating of powder metal-hydride systems.

(**a**)   (**b**)
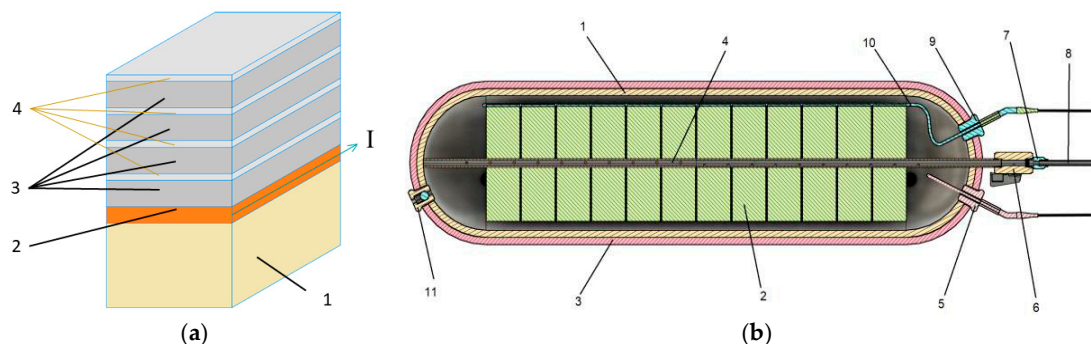
Figure 7. Film metal-hydride hydrogen accumulator: (**a**) structural scheme: 1—polyimide substrate; 2—resistive layer with current I; 3—magnesium film; 4—nickel film (catalyst); (**b**) constructive scheme: 1—liner; 2—winding of film hydride-formation material on a polymer substrate with a resistive layer; 3—case; 4—hollow winding roll; 5—temperature sensor; 6,7,8—gas puffing fitting; 9,10—electrical supply; 11—pressure-release valve.

5. Conclusions

Microscale periodic Ni-Mg-Ni-Mg film structures can be saturated by hydrogen to about the same percent content as volume powder materials (7.0–7.5 wt.%) but at lower pressures (~20–30 atm) and temperatures (200–250 °C). Hydrogen is also desorbed therefrom at lower temperatures (250–300 °C) with better kinetics and considerably lower values of heat spent for hydrogen output. An increase in the nickel content from 4 to 12 at.% with an increase in the ratio of the thicknesses of the nickel and magnesium layers in the periodic Ni-Mg-Ni-Mg film structures is accompanied with a decrease in the enthalpy of phase formation from 46.7 to 19.8 kJ/mol H_2. The significantly lower value of the enthalpy of phase formation in these films compared to the bulk material of the same composition may be a consequence of the amorphous nature of their structure and the developed "magnesium–nickel" contact interface in them. The maximum content of reversibly stored hydrogen obtained in the experiments was 3.4 wt.% at a hydrogen pressure of 1 atm and a desorption temperature of 300 °C.

Author Contributions: D.A.K.: organization of the workflow and preparation of the article; A.G.I.: study of the microstructure of samples, calorimetric studies, analysis of experimental results; E.S.C.: sorption–desorption experiments; M.I.Y.: deposition of periodic film structures, X-ray structural analysis. All authors have read and agreed to the published version of the manuscript.

Data Availability Statement: The data presented in this study are available on request from the corresponding author. The data are not publicly available due to their large number.

References

1. Bellosta von Colbe, J.; Ares, J.-R.; Barale, J.; Baricco, M.; Buckley, C.; Capurso, G.; Gallandat, N.; Grant, D.M.; Guzik, M.N.; Jacob, I.; et al. Application of hydrides in hydrogen storage and compression: Achievements, outlook and perspectives. *Int. J. Hydrogen Energy* **2019**, *44*, 7780–7808. [CrossRef]

2. Pistidda, C. Solid-State Hydrogen Storage for a Decarbonized Society. *Hydrogen* **2021**, *2*, 428–443. [CrossRef]
3. Kumar, A.; Muthukumar, P.; Sharma, P.; Kumar, E.A. Absorption based solid state hydrogen storage system: A review. *Sustain. Energy Technol. Assess.* **2022**, *52 Pt C*, 102204. [CrossRef]
4. Lin, H.-J.; Lu, Y.-S.; Zhang, L.-T.; Liu, H.-Z.; Edalati, K.; Révész, Á. Recent advances in metastable alloys for hydrogen storage: A review. *Rare Met.* **2022**, *41*, 1797–1817. [CrossRef]
5. Modi, P.; Aguey-Zinsou, K.-F. Room Temperature Metal Hydrides for Stationary and Heat Storage Applications: A Review. *Front. Energy Res.* **2021**, *9*, 616115. [CrossRef]
6. Corré, S.; Bououdina, M.; Kuriyama, N.; Fruchart, D.; Adachi, G.Y. Effects of mechanical grinding on the hydrogen storage and electrochemical properties of $LaNi_5$. *J. Alloys Compd.* **1999**, *292*, 166–173. [CrossRef]
7. Chandra, S.; Sharma, P.; Muthukumar, P.; Sarma V Tatiparti, S. Experimental hydrogen sorption study on a $LaNi_5$-based 5 kg reactor with novel conical fins and water tubes and its numerical scale-up through a modular approach. *Int. J. Hydrogen Energy* **2022**, *in press*. [CrossRef]
8. Jain, J.P.; Lal, C.; Jain, A. Hydrogen storage in Mg: A most promising material. *Int. J. Hydrogen Energy* **2010**, *35*, 5133–5144. [CrossRef]
9. Pasquini, L.; Sakaki, K.; Akiba, E.; Allendorf, M.D.; Alvares, E.; Ares, J.-R.; Babai, D.; Baricco, M.; Bellosta von Colbe, J.; Bereznitsky, M.; et al. Magnesium- and intermetallic alloys-based hydrides for energy storage: Modelling, synthesis and properties. *Prog. Energy* **2022**, *4*, 032007. [CrossRef]
10. Klyamkin, S.N. Metal-hydride magnesium-based compositions as materials for hydrogen accumulation. *Ross. Chim. Zhurnal* **2006**, *50*, 49–55. (In Russian)
11. Shelyapina, M.G. Structure, Stability and Dynamics of Multi-Component Metal Hydrides According to the Data of the Theory of Density Functional and Nuclear Magnetic Resonance. Dr. Sci, SPbGU, Saint Petersburg, Russia, 2018; pp. 91–160. (In Russian).
12. Shen, S.; Ouyang, L.; Liu, J.; Wang, H.; Yang, X.-S.; Zhu, M. In situ formed ultrafine metallic Ni from nickel (II) acetylacetonate precursor to realize an exceptional hydrogen storage performance of MgH_2-Ni-EG nanocomposite. *J. Magnes. Alloys* **2022**, *in press*.
13. Jain, I.P.; Vijay, Y.K.; Malhotra, L.K.; Uppadhyay, K.S. Hydrogen storage in thin film metal hydride—A review. *Int. J. Hydrogen Energy* **1988**, *13*, 15–23. [CrossRef]
14. Han, B.; Yu, S.; Wang, H.; Lu, Y.; Lin, H.-J. Nanosize effect on the hydrogen storage properties of Mg-based amorphous alloy. *Scripta Mater.* **2022**, *216*, 114736. [CrossRef]
15. Lider, A.; Kudiiarov, V.; Kashkarov, E.; Syrtanov, M.; Murashkina, T.; Lomygin, A.; Sakvin, I.; Karpov, D.; Ivanov, A. Hydrogen Accumulation and Distribution in Titanium Coatings at Gas-Phase Hydrogenation. *Metals* **2020**, *10*, 880. [CrossRef]
16. Baldi, A.; Gonzalez-Silveira, M.; Palmisano, V.; Dam, B.; Griessen, R. Destabilization of the Mg-H system through elastic constraints. *Phys. Rev. Lett.* **2009**, *102*, 226102. [CrossRef]
17. Gharavi, A.G.; Akyildiz, H.; Öztürk, T. Thickness effects in hydrogen sorption of Mg/Pd thin films. *J. Alloys Compd.* **2013**, *580* (Suppl. S1), S175–S178. [CrossRef]
18. Abdul Majid, N.A.; Watanabe, J.; Notomi, M. Improved desorption temperature of magnesium hydride via multi-layering Mg/Fe thin film. *Int. J. Hydrogen Energy* **2021**, *46*, 4181–4187. [CrossRef]
19. Zhang, L.; Ji, L.; Yao, Z.; Yan, N.; Sun, Z.; Yang, X.; Zhu, X.; Hu, S.; Chen, L. Facile synthesized Fe nanosheets as superior active catalyst for hydrogen storage in MgH_2. *Int. J. Hydrogen Energy* **2019**, *44*, 21955–21964. [CrossRef]
20. Suárez-Alcántara, K.; Palacios-Lazcano, A.F.; Funatsu, T.; Cabañas-Moreno, J.G. Hydriding and dehydriding in air exposed Mg-Fe powder mixtures. *Int. J. Hydrogen Energy* **2016**, *41*, 23380–23387. [CrossRef]
21. Stillesjö, F.; Ólafsson, S.; Hjörvarsson, B.; Karlsson, E. Hydride Formation in Mg/Ni-Sandwiches Studied by Hydrogen Profiling and Volumetric Measurements. *Z. Phys. Chem.* **1993**, *181*, 353–358. [CrossRef]
22. Chen, Y.; Dai, J.; Xie, R.; Song, Y. A first-principles study on interaction of Mg/Ni interface and its hydrogen absorption characteristics. *Surf. Sci.* **2016**, *649*, 133–137. [CrossRef]
23. Ivanov, A.G.; Karpov, D.A.; Chebukov, E.S.; Yurchenkov, M.I. Research of hydrogen saturation of magnesium and magnesium-aluminum films and the influence of a protective nickel coating on it. *J. Phys. Conf. Ser.* **2021**, *1954*, 012014. [CrossRef]
24. Catalog of Hydride-Forming Materials «Hydride Information Center (Hydpark) Search Result». Available online: https://www.hydrogen.energy.gov/ (accessed on 27 February 2020).
25. Kuzubov, A.A.; Eliseeva, N.S.; Krasnov, P.O.; Kuklin, A.V.; Kovaleva, E.A.; Kholtobina, A.S. Theoretical study of hydrogen sorption and diffusion on the surface and in the volume of Mg_2Ni intermetallide. *Fiz. Tverd. Tela* **2014**, *56*, 1970–1977. (In Russian)
26. Li, L.; Akiyama, T.; Yagi, J.-I. Activity and capacity of hydrogen storage alloy Mg_2NiH_4 produced by hydriding combustion synthesis. *J. Alloys Compd.* **2001**, *316*, 118–123. [CrossRef]
27. Karpov, D.A.; Litunovsky, V.N. Accumulator for Hydrogen Storage in Bound State and a Cartridge for Accumulator. Patent RU 2606301C2, 10 January 2017.
28. Karpov, D. Film metal-hydride hydrogen accumulators: Potentials, production methods, prospects for application. In Proceedings of the International Conference on Innovative Applied Energy, Oxford, UK, 14–15 March 2019; p. 38.